Max-Planck-Institut
für Mathematik
in den Naturwissenschaften
Leipzig

Experimental Demonstration of Observability and Operability of Robustness of Coherence

by

Wenqiang Zheng, Zhi-Hao Ma, Hengyan Wang,
Shao-Ming Fei, and Xinhua Peng

Preprint no.: 57 2018

Experimental Demonstration of Observability and Operability of Robustness of Coherence

Wenqiang Zheng,[1,*] Zhihao Ma,[2,*] Hengyan Wang,[3,†] Shao-ming Fei,[4,5,‡] and Xinhua Peng[6,7,8,§]

[1] *Center for Optics & Optoelectronics Research, Collaborative Innovation Center for Information Technology in Biological and Medical Physics, College of Science, Zhejiang University of Technology, Hangzhou 310023, China*

[2] *Department of Mathematics, Shanghai Jiaotong University, Shanghai 200240, China*

[3] *Department of Physics, Zhejiang University of Science and Technology, Hangzhou 310023, China*

[4] *School of Mathematical Sciences, Capital Normal University, Beijing 100048, China*

[5] *Max-Planck-Institute for Mathematics in the Sciences, 04103 Leipzig, Germany*

[6] *CAS Key Laboratory of Microscale Magnetic Resonance and Department of Modern Physics, University of Science and Technology of China, Hefei 230026, China*

[7] *Hefei National Laboratory for Physical Sciences at the Microscale, University of Science and Technology of China, Hefei 230026, China*

[8] *Synergetic Innovation Center for Quantum Effects and Applications (SICQEA), Hunan Normal University, Changsha 410081, China*

Quantum coherence is an invaluable physical resource for various quantum technologies. As a bona fide measure in quantifying coherence, the robustness of coherence (RoC) is not only mathematically rigorous, but also physically meaningful. We experimentally demonstrate the witness-observable and operational feature of the RoC in a multi-qubit nuclear magnetic resonance system. We realize witness measurements by detecting the populations of quantum systems in one trial. The approach may also apply to physical systems compatible with ensemble or nondemolition measurements. Moreover, we experimentally show that the RoC quantifies the advantage enabled by a quantum state in a phase discrimination task.

As an essential feature of quantum mechanics, quantum coherence is regarded as a precious resource that is not present in the classical world. It characterizes the quantumness and underpins quantum correlations in quantum systems. As quantum technologies are developing rapidly, quantum coherence is found to play a key role in many novel quantum phenomena and has been widely studied and applied in many quantum information processing tasks [1, 2, 3, 4, 5, 6, 7, 8, 9, 10, 11, 12, 13, 14, 15, 16, 17, 18].

The degree of coherence may quantify the capability of a quantum state in quantum-enhanced applications. To quantify the coherence, a set of quantifiers have been presented, which greatly enriches our understanding of coherence. The relative entropy and l_1-norm coherence measures are two well-known measures of coherence [1]. Other coherence measures like distillable coherence [19, 20], coherence of formation [19, 20, 21], coherence measures based on entanglement [10], and coherence concurrence [22, 23] have been also proposed and investigated. Moreover, the relations between coherence and path information [24, 25], the distribution of quantum coherence in multipartite systems [18], the complementarity between coherence and mixedness [26, 27] have also been studied.

To be a proper measure of coherence, the quantifier should meet a rigorous framework [1], such as monotonicity under incoherent operations. The relative entropy coherence [11] is a canonical measure. However, its experimental determination requires full state tomography, which is unfeasible for large systems. Recently, a bona fide measure, named robustness of coherence (RoC) [8], has been put forward. The RoC is a full monotone under all the sets of operations used in resource theories of coherence. It is observable and provides an alternative to the tomographic technique. Moreover, the RoC has a direct operational meaning that it quantifies the advantage enabled by a quantum state in a phase discrimination

task [8]. These characteristics make RoC attractive.

Let $\mathscr{D}$ be the convex set of density operators acting on a d-dimensional Hilbert space, and $\mathcal{S}$ the subset of incoherent states whose density matrices are diagonal in the reference basis. Defined by the minimal mixing required to destroy all the coherence in a quantum state ρ, the RoC is given by

$$\mathcal{C}(\rho) = \min_{\tau\in\mathcal{D}} \left\{ s \geq 0 \left| \frac{\rho + s\tau}{1+s} = \delta \in \mathcal{S} \right. \right\}, \tag{1}$$

which is the minimum weight of another state τ such that its convex mixture with ρ yields an incoherent state. Interestingly, for RoC one can introduce the coherence witness, which makes the RoC an *observable* quantity. For a given state, one can find its optimal witness W^* by a simple semidefinite program, making use of the free CVX package [8, 28]. The optimal witness saturates the inequality $\max\{0, -Tr[\rho W]\} \leq \mathcal{C}(\rho)$. Therefore, the RoC of the state can be quantified by the expected value of W^*, $\mathcal{C}(\rho) = -Tr(W^*\rho)$. In [29] the authors have presented a beautiful way in experimentally measuring the RoC of a one-qubit photon system via the interference fringes.

Most attractively, the RoC shows its operational interpretation in the following phase discrimination (PD) task. Alice prepares a two-qubit quantum state ρ which then enters into a black box. The black box encodes a phase on the input state ρ by implementing a unitary operation $U_\phi = \exp(iN\phi)$, where N is designed as $N = \sum_{j=0}^{3} j\,|j\rangle\langle j|$. The phase ϕ is the 'black' parameter, which maybe one of $\{\phi_k = 2\pi k/4\}_{k=0}^{3}$, each with a prior equal probability 1/4. The receiver's task is to guess correctly which phase ϕ was actually encoded in the state. For this purpose, one can perform a generalized measurement given by the measurement operators M_k ($\sum_{k=1}^{4} M_k = \mathbb{I}$) on the output state $\rho_{out} = U_\phi \rho U_\phi^\dagger$. The success probability is then given by

$$p(\rho) = \sum\nolimits_{k=1}^{4} Tr\left[U_{\phi_k}\rho U_{\phi_k}^\dagger M_k\right]\Big/4. \tag{2}$$

The optimal measurement which gives rise to the maximal success probability is of the form $M_k = \frac{1}{4}U_{\phi_k}(1-W^*)U_{\phi_k}^\dagger$ [8], where W^* is the optimal witness associated with the input state ρ. For incoherent states δ, the black box encodes nothing, since $U_\phi(\delta) = \delta$, and the success probability is just 1/4. The advantage achievable by introducing coherence can be quantified exactly by the RoC of the input state ρ,

$$\mathcal{A}(\rho) \equiv \frac{p_{succ}(\rho)}{p_{succ}(\delta)} = 1 + \mathcal{C}(\rho). \tag{3}$$

In the following we experimentally present the operational and observable meaning of RoC in a nuclear magnetic resonance (NMR) quantum system, and show the power of RoC in the above phase discrimination game by demonstrating the relation Eq.(3). For practical significance, we also quantify the lower bound of RoC from limited information of the system. The method adopted in our experiments is applicable to general quantum systems.

We employ the nuclear spin system, operated on a 400 MHz nuclear magnetic resonance (NMR) spectrometer, and use diethyl fluoromalonate as the sample dissolved in ^2H-labeled chloroform at 304 K. The ^{13}C nucleus is used as the probe qubit (labeled as qubit 1), serving as an information extractor of the measured system. The measured system consists of one ^{19}F nucleus and one ^1H nucleus (labeled as qubits 2 and 3). The Hamiltonian of the three-qubit system in the triple resonance rotating frame is given by $H = 2\pi \sum_{1\leq i\leq j\leq 3} J_{ij} I_z^i I_z^j$, where I_z is the spin angular momentum operator of the z-component, J_{ij} is the scalar coupling strength between spins i and j. The relevant parameters along with the molecular structure are shown in Ref. [30].

In the high temperature approximation, the state of a two-qubit NMR system can be written as $\rho_s = (1-\varepsilon)\,\mathbb{I}_4/4 + \varepsilon\Delta\rho_s$, where $\varepsilon \sim 10^{-5}$ denotes the polarization of the NMR system in our experimental condition and $\mathbb{I}_4$ denotes the 4×4 identity matrix. In many proof-of-principle experiments, the part of deviation density matrix $\Delta\rho_s$ is usually used for NMR quantum information processing, because all measurements and transformations don't affect the identity matrix. Quantum correlation has been proven to exist in NMR system at room temperature [31, 32, 33]. The purpose of this paper is to quantify another quantum resource, i.e., quantum coherence. The RoC of a genuine NMR mixed state can be determined from the experimentally detectable deviation density matrix in the leading order in ε, by the following

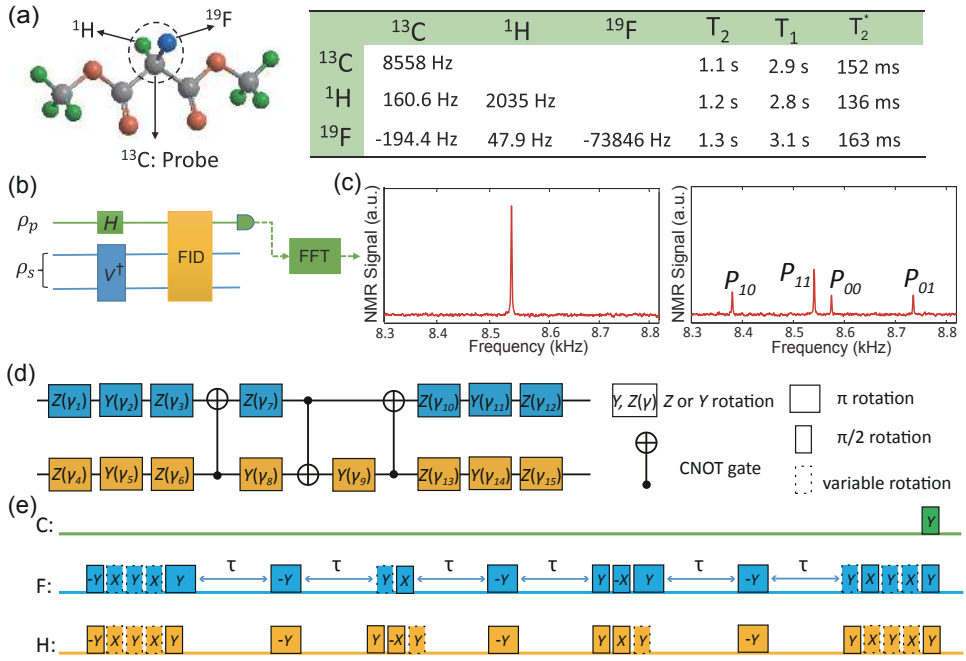

FIG. 1. Experimental methods and pulse sequences. (a) Quantum circuit for measuring $Tr\,(W\rho_s)$ in one trial. H: Hardmard gate, FID: free induction decay under the natural Hamiltonian, FFT: fast Fourier Transform. (b) ^{13}C spectra as examples for PPS state (left) and measured RoC (right). The area of each peak P_{ij} equals to the population of the spin state $|ij\rangle$. (c) An optimal quantum circuit for a general two-qubit gate in $\mathbf{U}(4)$. The circuit consists of 3 controlled-NOT (CNOT) gates and 15 elementary one-qubit gates. The 15 angles can be determined by a simple optimal search algorithm, making the circuit of almost perfect fidelity with the desired two-qubit operator. (d) Experimental process for the witness measurement of RoC. All the square pulses are hard pulses with negligible duration compared to the free evolution time $\tau=\frac{1}{4|J_{23}|}$.

equation [30]

$$\mathcal{C}\left(\rho_s\right)=\varepsilon\mathcal{C}\left(\Delta\rho_s\right). \tag{4}$$

Starting from the thermal equilibrium state, we firstly initialize the system in the pseudo-pure state $\Delta\rho_s = |00\rangle\langle 00|$ by using the line-selective method [34, 35], where $|0\rangle$, $|1\rangle$ represent the eigenvectors of the Pauli matrix σ_z. We first experimentally quantify the RoC of given states by the optimal coherence witness detection. To this end, we prepare the system (^{19}F nucleus and ^{1}H nucleus) in the form

$$\Delta\rho_s=\begin{pmatrix} 0.25 & b & a & a \\ b & 0.25 & b & a \\ a & b & 0.25 & b \\ a & a & b & 0.25 \end{pmatrix}. \tag{5}$$

Here we constrain a, b to real numbers and insure ρ is positive definite. The parameter region of a and b as well as the theoretical RoC of states of Eq. (5) are shown in Fig. 2(a). We can see that when $a = b = 0$ ($\Delta\rho_s$ is the maximally mixed state $\mathcal{I}$), $\mathcal{C}(\rho_s)$ is zero as expected, while when $a = b = 0.25$ ($\Delta\rho_s$ is the maximally coherent state $\mathcal{M}$), $\mathcal{C}\left(\rho_s\right)$ reaches the maximal value $\mathcal{C}(\rho_s) = 3\varepsilon$. As unitary controls alone can not realize the desired state transformation from the thermal equilibrium state, here we need to take use of nonunitary controls like gradient pulses to beforehand transform the eigenvalues of the state into desired values. Then A 'state-to-state' shape pulse based on the gradient ascent pulse engineering (GRAPE) algorithm [36] is utilized as a shortcut for a nearly perfect preparation, avoiding error accumulation and decoherence effect in conventional pulse sequence method.

Now we provide an experimental method to show the observability of RoC. The witness observable W^*, gained by the CVX package, can be diagonalized as $W^* = VDV^\dagger$, where D is the diagonal matrix with the eigen-

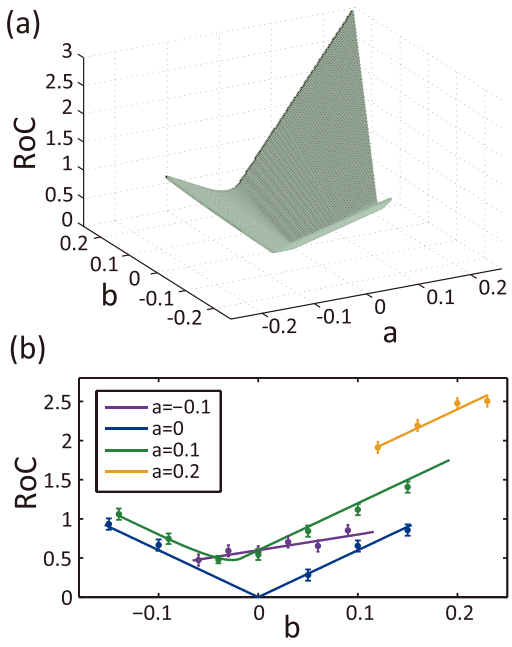

FIG. 2. (a) Theoretical values of RoC for states with deviation density matrices in the form of Eq. (5). (b) Experimentally measured results, compared with the theoretical values (solid curves). The coherences are displayed in units of ε.

values of W^* as diagonal elements, V is a unitary matrix whose columns are the eigenvectors. We then have

$$\mathcal{C}(\rho_s) = -\mathrm{Tr}(W^*\rho_s) = -\sum_{i=1}^{4} \rho_{ii}^{'} D_{ii}, \qquad (6)$$

where $\rho^{'} = V^{\dagger}\rho_s V$ and $\rho_{ii}^{'}$ is the spin population in the ith energy level. Therefore, we can measure the expected value of W^* by the circuit shown in Fig. 1b. That is, we implement the operation $V^{\dagger}$ on the system, and then measure the population distribution of the system, i.e. the diagonal elements of the density matrix. The RoC is finally calculated by Eq. (6). To implement the operator $V^{\dagger}$, an optimal quantum circuit for a general two-qubit gate in $\mathbf{U}(4)$ as the form of Fig. 1d is used [37].

To avoid non-uniformity and uncertainty in preparing copies of the state, here in our experiment, we utilize one probe qubit to measure the population distribution of the system directly in only one trial. As shown in Fig. 1(b), we firstly implement a Hardmard gate on ^{13}C to generate transverse polarization. Then the probe qubit interacts with system qubits through the free evolution under the natural Hamiltonian. During the evolution, we do NMR signal detection on the ^{13}C channel. Through Fourier transformation, we get the NMR spectra of ^{13}C, one of which is shown in Fig. 1c. There are four peaks in one ^{13}C spectrum and the area of each individual peak is proportional to the diagonal element of the corresponding energy level. In the situation where peaks of the spectrum are too dense to distinguish from each other, we can extract the desired information of peaks by fitting the spectrum, with prior knowledge of peak positions and line profiles (Lorenz curve is the best option for NMR spectra). We also can address this problem by adding ancillary qubits. π echo pulses are inserted during the free evolution, which significantly suppress the decoherence effect rooted in the inhomogeneity of the magnetic field. Hence the decoherence effect is depicted with the characteristic relaxation time T_2, rather than T_2^*. We numerically simulate the dynamical process and estimate the attenuation factors caused by decoherence effect in the experiments. Rescaling the experimental results, we obtain the measured RoC, see Fig. 2b, where the pulse errors and data fitting errors are responsible for the error bars.

We have experimentally demonstrated that it is feasible to measure the RoC via an optimal witness. However, one needs some particular knowledge of the state to determine the optimal witness. Actually, given the expectation values of a set of measured observables, one can get an optimal lower bound of RoC (LRoC) [8]. This is meaningful for witnessing coherence effects in actual quantum processing, especially in large-scale quantum systems. In the experiment, by firstly initializing the purity of the system to a random value and then implementing a random unitary operation, we prepare six random states. We choose the following sixteen complete base operators $o_0 \sim o_{15}$: $I\otimes I$, $I_x\otimes I$, $I\otimes I_x$, $I_x\otimes I_x$, $I_y\otimes I$, $I\otimes I_y$, $I_y\otimes I_y$, $I_x\otimes I_z$, $I_z\otimes I_x$, $I_y\otimes I_z$, $I_z\otimes I_y$, $I_x\otimes I_y$, $I_y\otimes I_x$, $I_z\otimes I$, $I\otimes I_z$, $I_z\otimes I_z$. For a subset of the base operators $\mathrm{O}_i = \{o_j\}_{j=0}^{i}$, $i = 1, ..., 15$, we consider the coherence witness of the form $W_i = \sum_{n=1}^{i} c_n o_n + m\mathbb{I}$, $c_n, m \in R$. Depending on the expectation values of O_i, we optimize the values of c_n, m by a semidefinite program and get the coherence witness for a lower bound of RoC, $LC_i(\rho_s) = -Tr(W_i\rho_s)$, which is experimentally

measured by the circuit shown in Fig. 1. The experimental results are presented in Fig. 3. We can see that the LRoC is improved when more expectation values of observables are taken into account. The gap between the lower bound and the exact value of RoC vanishes when all the base operators are considered.

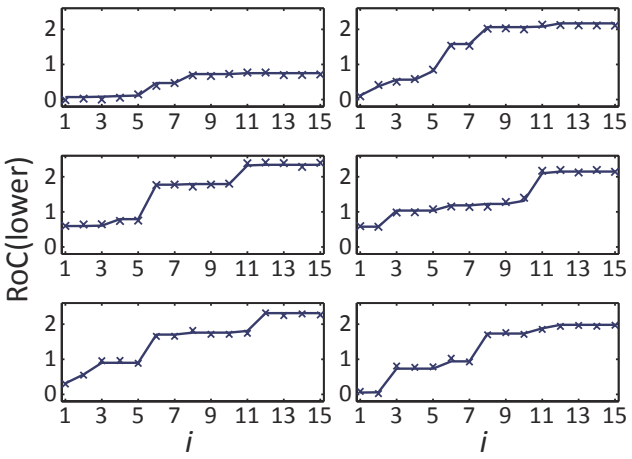

FIG. 3. Experimentally measured lower bound of RoC for random states, with different numbers of observables. Solid lines are theoretical values. The coherences are displayed in units of ε.

Having experimentally measured the RoC, we are now ready to show that RoC also plays roles in a metrology context via the previously described PD game. To experimentally verify it, we prepare a series of input states in the form,

$$\rho_g = (1+p)\frac{\mathcal{I}}{4} - p\rho_m. \tag{7}$$

They are mixtures of the state ρ_m ($p=-1$) and the maximally mixed state $\mathcal{I}$ ($p=0$) with the weight p, where ρ_m is the NMR state with $\Delta\rho_m = |\psi_m\rangle\langle\psi_m|$, $|\psi_m\rangle$ is the maximally coherent state, i.e., $|\psi_m\rangle = \frac{1}{2}\sum_{j=0}^{3}|j\rangle$. Then each U_{ϕ_k} is implemented by a GRAPE shape pulse. The probability with respect to the measurement operator M_k, i.e., $p_k = Tr\left(U_\phi \rho_{in} U_\phi^\dagger M_k\right)$, is measured by the similar circuit in Fig. 1(b). By Eq. (2), we obtain the success probability corresponding to the related input state in the game. The experimental results of the advantage against the incoherent case are shown in Fig. 4. As expected, the advantage vanishes when RoC is zero. The advantages coincide well with the RoC of the investigated states and the practical meaning of the RoC is well verified in the quantum game experiment.

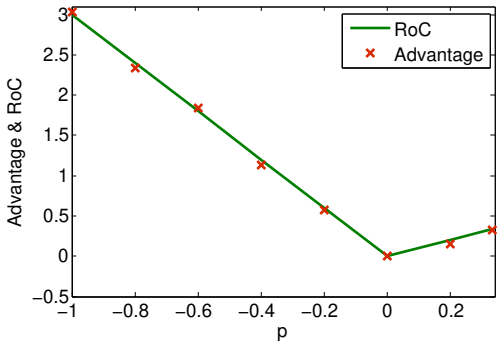

FIG. 4. Advantage gained in PD quantum game against the incoherent case. The data are displayed in units of ε.

In conclusion,the operational and observable meaning of RoC have been experimentally demonstrated by using an NMR quantum system. By experimentally verifying the relation between RoC and the maximal success probability given from coherent and incoherent states in PD games, the power of RoC in phase discrimination processing has been explicitly displayed. In the experiment, we extracted the expectation value of the witness observable from the population distribution of the quantum system. We utilized one ancillary qubit as a probe qubit to measure the population distribution directly in one trial, avoiding full state tomography, as well as the non-uniformity and uncertainty in state preparing. By using this method, we can simplify observable measurements for the systems compatible with ensemble measurements (where the population distribution can be measured in one trial) or nondemolition measurements (where the population distribution can be repeatedly measured without state re-preparation) [38]. In addition, we have also quantified the lower bound of RoC from limited information of the system. Many experimental investigations in many-body quantum systems may benefit from this technique for coherence estimation. The witness operators of quantum coherence are found by a semidefinite program at present. In following study, we expect to find unified forms of witness observables, as well as the related circuits for states with specific forms, such as X-shaped density matrix (which contain in particular Bell diagonal states of two qubits).

Acknowledgments This work is supported by National Natural Science Foundation of China (Grants No. 11605153, 11661161018, 11375167, 11227901, 11675113, 11275131 and 11571313), National Key Basic Research Program of China (2013CB921800, 2014CB848700), National Science Fund for Distinguished Young Scholars of China (Grant No. 11425523), the Strategic Priority Research Program (B) of the CAS (Grants No. XDB01030400).

* These authors contributed equally to this work.
† hywang@zust.edu.cn
‡ feishm@cnu.edu.cn
§ xhpeng@ustc.edu.cn

[1] T. Baumgratz, M. Cramer, and M. B. Plenio, Phys. Rev. Lett. **113**, 140401 (2014). 1
[2] A. Streltsov, S. Rana, P. Boes, and J. Eisert, Phys. Rev. Lett. **119**, 140402 (2017). 1
[3] A. Streltsov, S. Rana, M. N. Bera, and M. Lewenstein, Phys. Rev. X **7**, 011024 (2017). 1
[4] A. Streltsov, G. Adesso, M. B. Plenio, arXiv:1609.02439. 1
[5] M. L. Hu, X. Y. Hu, Y. Peng, Y. R. Zhang, and H. Fan, arXiv:1703.01852. 1
[6] T. R. Bromley, M. Cianciaruso, and G. Adesso, Phys. Rev. Lett. **114**, 210401 (2015). 1
[7] D. Girolami, Phys. Rev. Lett. **113**, 170401 (2014). 1
[8] C. Napoli, T. R. Bromley, M. Cianciaruso, M. Piani, N. Johnston, and G. Adesso, Phys. Rev. Lett. **116**, 150502 (2016). 1, 2, 4
[9] J. Ma, B. Yadin, D. Girolami, V. Vedral, and M. Gu, Phys. Rev. Lett. **116**, 160407 (2016). 1
[10] A. Streltsov, U. Singh, H. S. Dhar, M. N. Bera, and G. Adesso, Phys. Rev. Lett. **115**, 020403 (2015). 1
[11] A. Winter, and D. Yang, Phys. Rev. Lett. **116**, 120404 (2016). 1
[12] E. Chitambar, A. Streltsov, S. Rana, M. N. Bera, G. Adesso, and M. Lewenstein, Phys. Rev. Lett. **116**, 070402 (2016). 1
[13] E. Chitambar, and M. H. Hsieh, Phys. Rev. Lett. **117**, 020402 (2016). 1
[14] E. Chitambar, and Gilad Gour, Phys. Rev. Lett. **117**, 030401 (2016). 1
[15] I. Marvian, R. W. Spekkens, and P. Zanardi, Phys. Rev. A **93**, 052331 (2016). 1
[16] Y. Yao, X. Xiao, L. Ge, and C. P. Sun, Phys. Rev. A **92**, 022112 (2015). 1
[17] M. Piani, M. Cianciaruso, T. R. Bromley, C. Napoli, N. Johnston, and G. Adesso, Phys. Rev. A **93**, 042107 (2016). 1
[18] C. Radhakrishnan, M. Parthasarathy, S. Jambulingam, and T. Byrnes, Phys. Rev. Lett. **116**, 150504 (2016). 1
[19] A. Winter and D. Yang, Phys. Rev. Lett. **116**, 120404 (2016). 1
[20] X. Yuan, H. Zhou, Z. Cao, and X. Ma, Phys. Rev. A **92**, 022124 (2015). 1
[21] J. Aberg, arXiv: quant-ph/0612146. 1
[22] X. F. Qi, T. Gao, and F. L. Yan, J. Phys. A: Math. Theor.**50**, 285301(2017). 1
[23] S. P. Du, Z. F. Bai, and X. F. Qi, Quantum Inf. Comput. **15**, 1307(2015). 1
[24] M. N. Bera, T. Qureshi, M. A. Siddiqui, and A. K. Pati, Phys. Rev. A **92**, 012118 (2015). 1
[25] E. Bagan, J. A. Bergou, S. S. Cottrell, and M. Hillery, Phys. Rev. Lett. **116**, 160406 (2016). 1
[26] S. Cheng and M. J. W. Hall, Phys. Rev. A **92**, 042101 (2015). 1
[27] U. Singh, M. N. Bera, H. S. Dhar, and A. K. Pati, Phys. Rev. A **91**, 052115 (2015). 1
[28] M. Grant and S. Boyd, CVX: Matlab software for disciplined convex programming, version 2.1, http://cvxr.com/cvx (2014). 2
[29] Y. T. Wang et al., Phys. Rev. Lett. **118**, 020403 (2017). 2
[30] See Supplemental Material. 2, 3
[31] R. Auccaise et al., Phys. Rev. Lett. **107**, 070501 (2011). 2
[32] I. Silva *et al.*, Phys. Rev. Lett. **110**, 140501 (2013). 2
[33] D. O. Soares-Pinto *et al.*, Phys. Rev. A **81**, 062118 (2010). 2
[34] N. A. Gershenfeld and I. L. Chuang, Bulk Spin-Resonance Quantum Computation, Science **275**, 350 (1997). 3
[35] X. Peng, X. Zhu, X. Fang, M. Feng, K. Gao, X. Yang, and M. Liu, Chem. Phys. Lett. **340**, 509 (2001). 3
[36] N. Khaneja, T. Reiss, C. Kehlet, T. Schulte-Herbruggen, and S. J. Glaser, J. Magn. Reson. **172**, 296 (2005). 3
[37] F. Vatan and C. Williams, Phys. Rev. A **69**, 032315 (2004). 4
[38] A. A. Clerk et al., Rev. Mod. Phys. **82**, 1155 (2010). 5